COBEM 2023 27TH INTERNATIONAL CONGRESS OF MECHANICAL ENGENEERING

ABCM Brazilian Society of Mechanical Sciences and Engineering
27th ABCM International Congress of Mechanical Engineering
December 04-08, 2023, Florianópolis-SC, Brazil

# COB-2023-1146
# ANALYSIS OF THE SUSPENSION ENERGY HARVESTING POTENTIAL BY MEANS A 9 DOF NON-LINEAR TRUCK MODEL

**Augusto Schmidt Lenz**
**João Gabriel Benedito Duarte**
**Mariana Damm Poli**
**Eduardo André Perondi**
Universidade Federal do Rio Grande do Sul – Laboratório de Mecatrônica e Controle, Rua Sarmento Leite, 425, Sala 204 – Centro Histórico, Porto Alegre – RS, CEP 90050-170.
augusto.lenz@ufrgs.br, joao.benedito@ufrgs.br, mariana.poli@ufrgs.br, eduardo.perondi@ufrgs.br

***Abstract.*** *Currently, regenerative vehicle suspensions consist of a widely studied field of research. These systems are capable of collecting energy from motor vehicle suspensions, which would normally be wasted through heat dissipation. The present work aims to analyze the responses of dynamic simulation of typical suspension trucks in order to evaluate the potential of energy available to be collected. With this target, a detailed mathematical model was developed considering a 9 degrees of freedom (DOF) model. The phase differences of the excitation signals for each of the axes are considered from the horizontal distances between the axes and the translation speed considered in the simulations. The vertical movement of each wheel is calculated according to a speed profile of the truck being used to determine the angle of inclination that occurs in a situation of braking or acceleration of the vehicle, for instance. A simulation model was programmed in the MATLAB/Simulink system using typical parameters of these systems. In the simulation model, the stiffness and damping behaviors are defined by vendor datasheets, using even nonlinear curves of commercial components when available. The road profiles are calculated according to ISO 8608:2016, considering the types of roads A, B and C, which have been defined as operational cases of these systems. With the results of the simulations obtained, an analysis of the forces, speeds, displacements and available energy potential is performed, allowing to determine the most important excitation frequencies suitable for the capture of energy, maximum and average values of force, speed, energy power and the amplitude of the oscillation between the suspensions of different axes, highlighting the conditions in which the use of a regenerative suspension would be more suitable to energy regeneration purposes. These parameters can be used to compare different energy harvesting systems, since the maximum potential obtained via simulation can be used as a reference for the maximum energy available in a given type of suspension. This work aims to demonstrate the use of a nonlinear mathematical model of a truck with 9 DOF in MATLAB/SIMULINK for sizing the harvesting capacity of a regenerative suspension using the ISO 8608:2016 standard as a road profile generator.*

***Keywords:*** *Truck Suspension, Energy Harvesting, ISO 8608:2016, Simulink, Numerical Simulation*

## 1. INTRODUCTION

In the automotive industry, every reuse of energy is extremely important to vehicular autonomy. Nowadays, trucks are increasingly costly in terms of energy, mainly due to the increase of the driver and passenger's comfort. In addition to energy consumption coming from the cockpit, is observed an increasing evolution in the use of electrical vehicles which need energy sources of high volume and high value and low autonomy. With this problem in mind, many different forms of embedded regeneration in vehicles to increase the energy source have been proposed. Warake et al. (2018) indicates a regeneration system through vehicular braking, in order that during the retarded process of the automobile, a motive force is created in the axles with auxiliar motors, in a way that the energy can be withdrawal of this system and later be used to the aid of traction of hills, or, in the case of purely electrical vehicles, during every part of the traject. Other regenerative methods are being studied, as shown by Zou et al. (2017) in his survey about regenerative suspension. The idea of this system is to use the mechanic energy dissipated by the dampers of a vehicular suspension transforming it into hydraulic energy thought a piston and, later, transmit a hydraulic energy, through a hydraulic motor in rotation, providing, then, the engagement of the electrical generator. Considering this possibility, a quarter of car models have already been explored by Zuo et al. (2013) and Liu et al. (2016), who discovered values of axle power by axle between 10 and 1626 Watts. With this information, this article develops a model of 9 DOF applied to *Simulink* with non-linear parameters, in order to obtain results more precise in relation to the existent ones.

In the automotive industry, energy reuse is extremely important for vehicle autonomy. Nowadays, trucks are becoming increasingly energy-consuming, mainly due to the increased comfort for the driver and passengers. In addition to the energy consumption in the cockpit, there is a growing trend towards the use of electric vehicles that require high-volume, high-value, and low-autonomy energy sources. With this problem in mind, various forms of energy regeneration incorporated into vehicles have been proposed. Warake et al. (2018) suggests a regeneration system through vehicle braking, where during the deceleration process of the vehicle, a driving force is created in the axles with auxiliary motors. This energy can then be extracted from the system and used to assist in uphill traction or, in the case of purely electric vehicles, throughout the entire journey. Other regenerative methods are also being studied, as shown by Zou et al. (2017) in their research on regenerative suspension. The idea of this system is to utilize the mechanical energy dissipated by the vehicle suspension dampers, transforming it into hydraulic energy through a piston, and then transmitting hydraulic energy through a rotating hydraulic motor, thereby coupling it to an electric generator. Considering this possibility, a quarter of the car models have already been explored by Zuo et al. (2013), as well as Liu et al. (2016), who discovered power values per axle ranging from 10 to 1626 Watts. With this information, this article develops a 9 DOF model applied to Simulink with nonlinear parameters in order to obtain more accurate results compared to existing ones.

## 2. MATHEMATICAL MODEL

Considering a 9 DOF model, a rigid body equilibrium approach was used to develop the dynamic equation set. The model is structured taking into account the mass of the vehicle body connected to six others masses that represent each wheel axles of the truck. Between each axle and the mass of the body are arranged a shock absorber and a suspension spring. The effect of tires is considered by means of a linear spring, and its dissipative effect is disregarded. A schematic diagram of the model is represented in Figure 1.

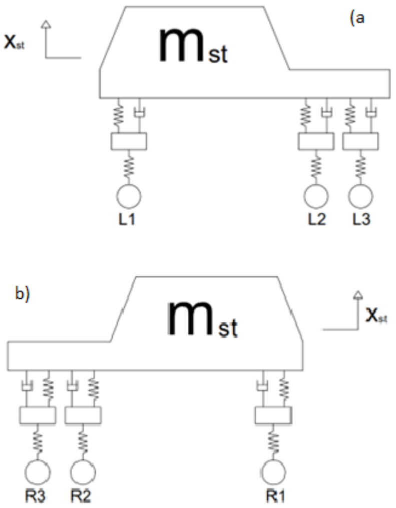


Figure 1. Diagram of the truck mechanical system, (a)right side and (b)left side.

The model shown in Figure 1 represents two lateral views, being therefore part of the complete drawing, since the vehicle has 6 independent suspension sets, denominated L1, L2, L3, R1, R2 and R3, in which the first three refer to its left side and the last three to its right side. Model details of each suspension system are shown in Figure 2, where each component is properly named.

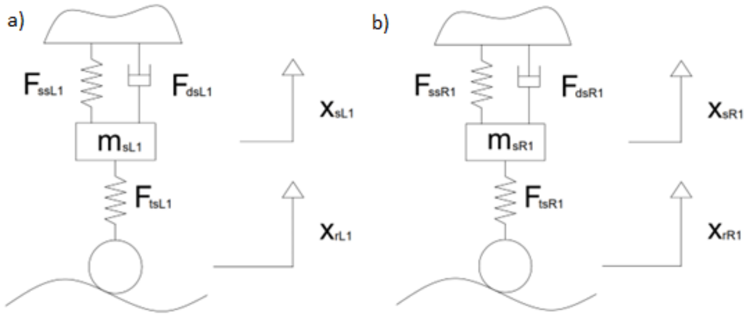


Figure 2. Diagram of front (a)left and (b)right suspensions.

The values of the spring elastic forces are called FssL1 for the L1 suspension assembly, FssL2 for the L2 suspension assembly, and FssL3 for the L3 suspension assembly. The same classification standard is used for the other mechanical components of each suspension assembly. More information about each component is presented in Table 1.

In the truck model previously described, the masses are considered restricted to the unidirectional vertical movement of translation, so that they move exclusively in the direction of compression and traction of the shock absorber and the spring of the suspension, so that each mass of the suspension has only 1 DOF. The mass of the main vehicle body is appropriately described by three DOF, one translational and the other rotational (pitch and roll). Thus, considering known the movements of the degrees of freedom relative to the tires, nine independent equations are needed to describe the dynamic behavior of the system. The sum of the forces in the vertical direction is given by Equation 1.

$$m_{st}\ddot{x}_{st} = -F_{ssL1} - F_{dsL1} - F_{ssL2} - F_{dsL2} - F_{ssL3} - F_{dsL3} - F_{ssR1} - F_{dsR1} - F_{ssR2} - F_{dsR2} - F_{ssR3} - F_{dsR3} \quad (1)$$

The sum of moments is given in two directions, one in y axis and the other in the z axis, the first indicates pitch while the second determines roll determined by the Equations 1 and 2:

$$\begin{aligned} I_{yyt}\ddot{\theta}_{st} = {} & -a(F_{ssL1} + F_{dsL1} + F_{ssR1} + F_{dsR1}) + b(F_{ssL2} + F_{dsL2} + F_{ssR2} + F_{dsR2}) \\ & + c(F_{ssL3} + F_{dsL3} + F_{ssR3} + F_{dsR3}) + h_{st}m_{st}\dot{v}_v \end{aligned} \quad (2)$$

$$I_{zzt}\ddot{\emptyset}_{st} = l(F_{ssL1} + F_{dsL1} + F_{ssL2} + F_{dsL2} + F_{ssL3} + F_{dsL3} - F_{ssR1} - F_{dsR1} - F_{ssR2} - F_{dsR2} - F_{ssR3} - F_{dsR3}) \quad (1)$$

Suspension masses only have forces in the vertical direction, resulting in the equations 4-9, as follows:

$$m_{sL1}\ddot{x}_{sL1} = F_{ssL1} + F_{dsL1} + F_{tsL1} \quad (2)$$

$$m_{sL2}\ddot{x}_{sL2} = F_{ssL2} + F_{dsL2} + F_{tsL2} \quad (3)$$

$$m_{sL1}\ddot{x}_{sL3} = F_{ssL3} + F_{dsL3} + F_{tsL3} \quad (4)$$

$$m_{sD1}\ddot{x}_{sD1} = F_{ssD1} + F_{dsD1} + F_{tsD1} \quad (5)$$

$$m_{sD2}\ddot{x}_{sD2} = F_{ssD2} + F_{dsD2} + F_{tsD2} \quad (6)$$

$$m_{sD1}\ddot{x}_{sD3} = F_{ssD3} + F_{dsD3} + F_{tsD3} \quad (7)$$

Vertical forces applied by mean the tires are described using equations 10-15:

$$F_{tsL1} = k_t(x_{rL1} - F_{tsL1}) \quad (8)$$

$$F_{tsL2} = k_t(x_{rL2} - F_{tsL2}) \quad (9)$$

$$F_{tsL3} = k_t(x_{rL3} - F_{tsL3}) \quad (10)$$

$$F_{tsD1} = k_t(x_{rD1} - F_{tsD1}) \quad (11)$$

$$F_{tsD2} = k_t(x_{rD2} - F_{tsD2}) \quad (12)$$

$$F_{tsD3} = k_t(x_{rD3} - F_{tsD3}) \quad (13)$$

The dissipative forces on the dumpers and the restitutive elastic forces on the air springs are nonlinear and depend directly on the speed and displacement, respectively. The displacement and velocity expressions of each suspension system for the L1 suspension system are presented in equations 16-33.

$$F_{ssL1} = f(\Delta x_{rsL1}), F_{dsL1} = f(\Delta \dot{x}_{rsL1}) \quad (14)$$

$$\Delta x_{rsL1} = x_{st} - x_{sL1} - \theta_{st}a + \emptyset_{st}l \quad (15)$$

$$\Delta \dot{x}_{rsL1} = \dot{x}_{st} - \dot{x}_{sL1} - \dot{\theta}_{st}a + \dot{\emptyset}_{st}l \quad (16)$$

For suspension system L2:

$$F_{ssL2} = f(\Delta x_{rsL2}), F_{dsL2} = f(\Delta \dot{x}_{rsL2}) \tag{17}$$

$$\Delta x_{rsL2} = x_{st} - x_{sL2} + \theta_{st} b + \emptyset_{st} l \tag{18}$$

$$\Delta \dot{x}_{rsL2} = \dot{x}_{st} - \dot{x}_{sL2} + \dot{\theta}_{st} b + \dot{\emptyset}_{st} l \tag{19}$$

For suspension system L3:

$$F_{ssL3} = f(\Delta x_{rsL3}), F_{dsL3} = f(\Delta \dot{x}_{rsL3}) \tag{20}$$

$$\Delta x_{rsL3} = x_{st} - x_{sL3} + \theta_{st} c + \emptyset_{st} l \tag{21}$$

$$\Delta \dot{x}_{rsL3} = \dot{x}_{st} - \dot{x}_{sL3} + \dot{\theta}_{st} c + \dot{\emptyset}_{st} l \tag{22}$$

For suspension system R1:

$$F_{ssR1} = f(\Delta x_{rsR1}), F_{dsR1} = f(\Delta \dot{x}_{rsR1}) \tag{23}$$

$$\Delta x_{rsR1} = x_{st} - x_{sR1} - \theta_{st} a - \emptyset_{st} l \tag{24}$$

$$\Delta \dot{x}_{rsL1} = \dot{x}_{st} - \dot{x}_{sR1} - \dot{\theta}_{st} a - \dot{\emptyset}_{st} l \tag{25}$$

For suspension system R2:

$$F_{ssR2} = f(\Delta x_{rsR2}), F_{dsR2} = f(\Delta \dot{x}_{rsR2}) \tag{26}$$

$$\Delta x_{rsR2} = x_{st} - x_{sR2} + \theta_{st} b - \emptyset_{st} l \tag{27}$$

$$\Delta \dot{x}_{rsR2} = \dot{x}_{st} - \dot{x}_{sR2} + \dot{\theta}_{st} b - \dot{\emptyset}_{st} l \tag{28}$$

For suspension system R3:

$$F_{ssR3} = f(\Delta x_{rsR3}), F_{dsR3} = f(\Delta \dot{x}_{rsR3}) \tag{29}$$

$$\Delta x_{rsR3} = x_{st} - x_{sR3} + \theta_{st} c - \emptyset_{st} l \tag{30}$$

$$\Delta \dot{x}_{rsR3} = \dot{x}_{st} - \dot{x}_{sR3} + \dot{\theta}_{st} c - \dot{\emptyset}_{st} l \tag{31}$$

Where the variables and parameters are correctly described in Table 1 and 2.

Table 1. System variables.

| **Variables** | **Meaning** |
|---|---|
| $x_{st}$ | X axis position of the suspense mass |
| $\theta_{st}$ | Y axis rotation of the suspense mass |
| $\emptyset_{st}$ | Z axis rotation of the suspense mass |
| $x_{sL1}, x_{sL2}, x_{sL3}, x_{sR1}, x_{sR2}, x_{sR3}$ | Position of the non-suspense masses |
| $\Delta x_{rsL1}, \Delta x_{rsL2}, \Delta x_{rsL3}, \Delta x_{rsR1}, \Delta x_{rsR2}, \Delta x_{rsR3}$ | Relative position of the suspensions |
| $x_{rL1}, x_{rL2}, x_{rL3}, x_{rR1}, x_{rR2}, x_{rR3}$ | Position of the tire applied by the road profile |
| $F_{ssL1}, F_{ssL2}, F_{ssL3}, F_{ssR1}, F_{ssR2}, F_{ssR3}$ | Forces applied by the springs of the suspension |
| $F_{dsL1}, F_{dsL2}, F_{dsL3}, F_{dsR1}, F_{dsR2}, F_{dsR3}$ | Forces applied by the dampers of the suspension |
| $v_v$ | Linear velocity of the vehicle |

Table 2. System parameters.

| **Parameters** | **Meaning** |
|---|---|
| $m_{st}$ | Mass of the suspense mass |
| $I_{yyt}$ | Moment of inertia in the y axis of the suspense mass |

| | |
|---|---|
| $I_{zzt}$ | Moment of inertia in the z axis of the suspense mass |
| $m_{sL2}, m_{sL2}, m_{sL3}, m_{sR2}, m_{sR2}, m_{sR3}$ | Masses of the suspensions |
| $a$ | Distance between L1 and R1 to the center of rotation of the suspense mass in the z axis |
| $b$ | Distance between L2 and R2 to the center of rotation of the suspense mass in the z axis |
| $c$ | Distance between L3 and R3 to the center of rotation of the suspense mass in the z axis |
| $l$ | Distance between all suspensions to the center of rotation of the suspense mass in the y axis |
| $h_{st}$ | Initial height between the center of mass of the system and the road |
| $k_t$ | Spring constant related to the tire |

In the pitch direction equation, the term $h_{st} m_{st} \dot{v}_v$ represents the momentum given by the acceleration of the vehicle in the direction of the linear movement, simulating the action of the vehicle during an accelerated or braking movement. The force values of air springs and nonlinear dumpers are determined from data of commercial components, being included in the simulation through lookup tables, which works by interpolating previously specified data. The tire vertical velocity related to the road profile is determined according to the ISO 8608:2016 and is imposed to the system by means an array of vertical movement synchronized with the horizontal position, allowing different excitation by axle due to the distance between rear and frontal axles.

ISO 8608:2016 Standard characterizes each road profile according to the power spectral density of the vertical road surface effect, separating in levels of frequencies and amplitudes considering increasing amplitudes in groups described from A to H, where A is related to the least rough road surface and H the higher situation.

### *2.1* Model in *Matlab Simulink*

To validate the model described, a block diagram was made in *Simulink* (Figure 3), and a script was created in *Matlab* to impose the parameters of the simulation. As already mentioned, the input signal for the road profile is determined correspondingly to ISO 8608:2016 and is imported to the simulation via an array of vertical by horizontal displacement. The linear velocity is integrated as another array that can be defined by the operator of the model, different tests were conducted with constant and variable velocities to demonstrate the effects. All other parameters values are described in Table 3.

To validate the described model, a block diagram was programmed in Simulink, and a script was created in Matlab to enforce the parameters of the simulation. As already mentioned, the input signal for the road profile is determined according to ISO 8608:2016 Standard and is imported into the simulation through a vertical by horizontal displacements matrix. Different tests were performed with constant and variable reference speeds. Other parameter values are described in Table 3.

Table 3. Values of the parameters for simulation.

| **Parameters** | **Value** |
|---|---|
| $m_{st}$ | 1900 kg |
| $I_{yyt}$ | 65158 kgm$^2$ |
| $I_{zzt}$ | 1945 kgm$^2$ |
| $m_{sL2}, m_{sL2}, m_{sL3}, m_{sR2}, m_{sR2}, m_{sR3}$ | 175 kg |
| $a$ | 1,5 m |
| $b$ | 2,0 m |
| $c$ | 3,25 m |
| $l$ | 1,25 m |
| $h_{st}$ | 1,5 m |
| $k_t$ | 9990000 N/m |

Force *versus* displacement data used for the nonlinear air spring of the suspension system, given by the WBD 500 Weforma air spring charged with 3 Bar of initial pressure, and the force *versus* velocity data used for the suspension nonlinear damper, presented by Bakar et al. (2008) are shown in Figure 4.

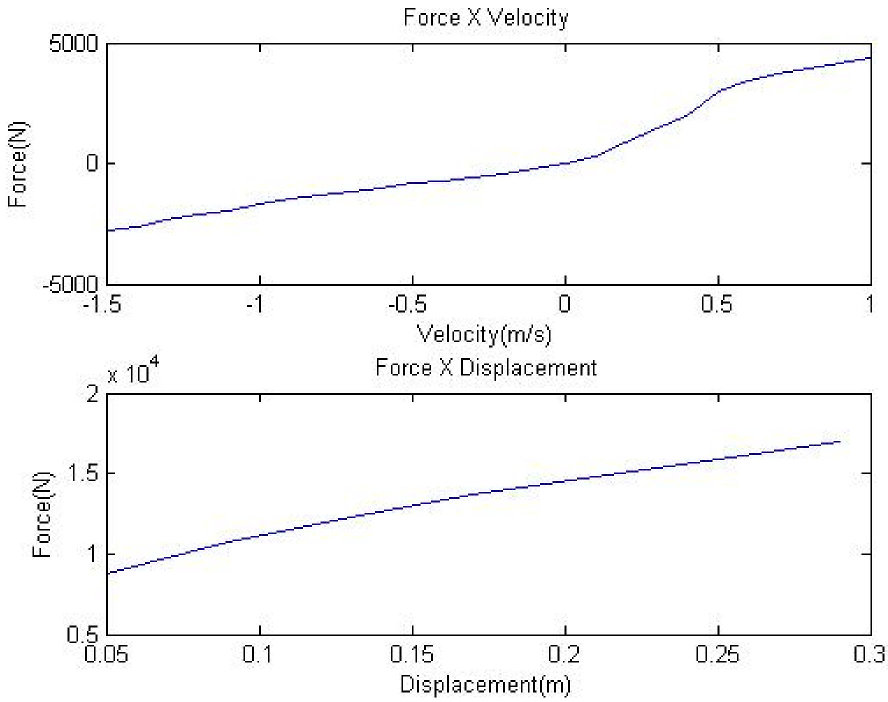


Figure 4. Force of air spring over displacement and force of damper over velocity.

Different simulations were performed using road profiles A, B and C, along with braking and acceleration situations of the vehicle in order to determine the power available by the suspension system. For each road profile, simulations were performed with 10, 20 and 30 m/s of linear speed, and the RMS values of available power on each of the axles were calculated along with the total power of the vehicle, as shown in Table 4.

Table 4. Results of RMS power from the simulation.

| | RMS power (W) | | | | | |
|---|---|---|---|---|---|---|
| | Road A | | Road B | | Road C | |
| **Velocity** | **Axle** | **Truck** | **Axle** | **Truck** | **Axle** | **Truck** |
| 10 m/s | 55,78 | 228,63 | 244,76 | 988,24 | 934,21 | 3841,2 |
| 20 m/s | 129,12 | 561,11 | 558,46 | 2404,3 | 1996,4 | 8948,5 |
| 30 m/s | 192,91 | 832,9 | 811,62 | 3472,5 | 3034,8 | 13772 |

Assuming a type B road profile, with the vehicle moving at 20 m/s, the power graphs over time for all six axles are shown in Figures 5-7.

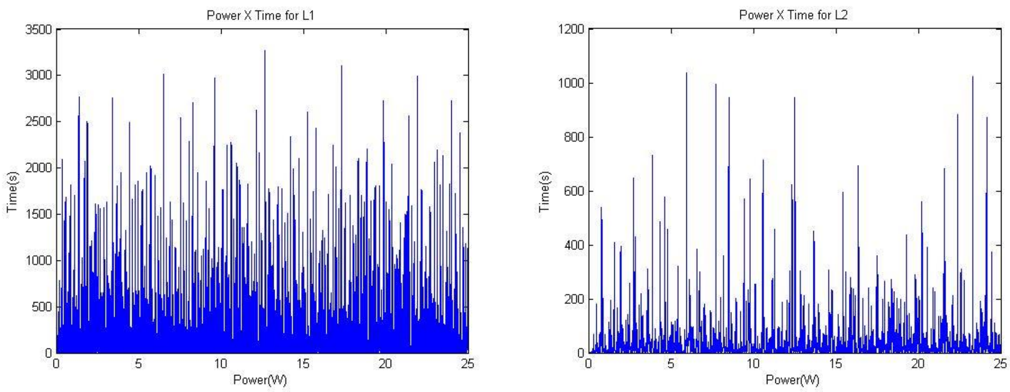


Figure 5. Power overtime for the L1 and L2 axles.

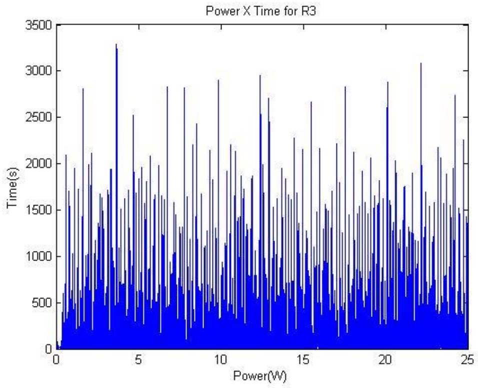


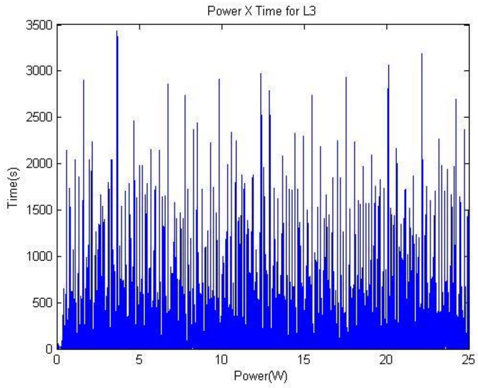


Figure 6. Power overtime for the L3 and R3 axles.

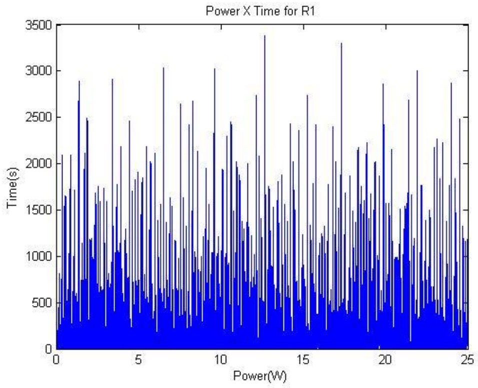


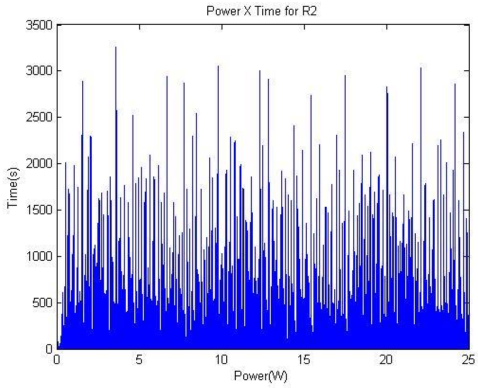


Figure 7. Power overtime for the R1 and R2 axles.

According to the figures shown above it is possible to identify a high oscillation in the power available, which can be easily understood by the determination of mechanical power, given that is a multiplication between force and velocity and the damper increases the force proportionally to the velocity.

The road profile for each axle is plotted in Figure 8.

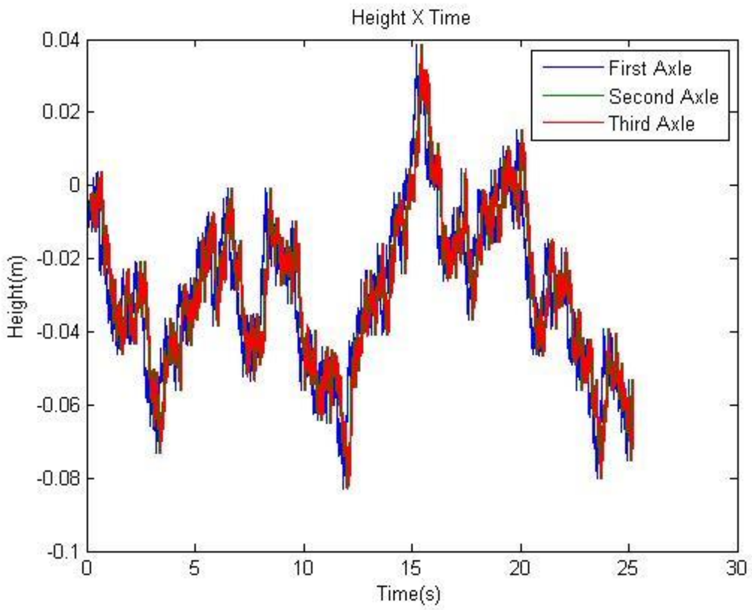


Figure 8. Height overtime for every axle.

Most models used for analysis of energy harvesting potential don't apply the phase between signals on each axle of the vehicle, which causes a big difference in the result. Data from a simulation with the same parameters used to generate Table 4, but without the phase, are shown in Table 5.

Table 5. Results of RMS power from the simulation without phase.

| | **RMS power (W)** | | | | | |
|---|---|---|---|---|---|---|
| | **Road A** | | **Road B** | | **Road C** | |
| **Velocity** | **Axle** | **Truck** | **Axle** | **Truck** | **Axle** | **Truck** |
| 10 m/s | 55,94 | 308,14 | 244,81 | 1352,8 | 934,87 | 5221,5 |
| 20 m/s | 131,33 | 724,1 | 568,15 | 3151,8 | 2029,3 | 11381 |
| 30 m/s | 196,24 | 1083,7 | 824,77 | 4591 | 3034,4 | 17040 |

The results presented demonstrate a small difference from the simulation considering the phase between axles, for smaller velocities, but it gradually increases accordingly to the velocity.

## 3. CONCLUSIONS

Analyzing the results obtained from simulations of the 9 DOF model, is easily concluded that for a regenerative damper model applied in all the axles from a Truck the energy harvesting potential rates between 0 and 14000 Watts. Furthermore, this value can be visibly changed, in simulation, according to a better modelling of the real system, which is shown in the comparation of Table 4 and Table 5, where the assumption of phase in the signal from the road changes up to 37% of the total power available in Truck suspension. Overall the data acquired proof that harvesting energy from a damper can be an efficient way of increasing autonomy of electric vehicles, as long as the regenerative system designed respects the responses of the non-linearity from the component in use, since we want to maintain the comfort of the passenger while harvesting energy.

## 4. ACKNOWLEDGEMENTS

The authors would like to thank Universidade Federal do Rio Grande do Sul - UFRGS and Laboratório de Mecatrônica e Controle - LAMECC for their support in the development of this work.

## 5. REFERENCES

Bakar, S. A. A., Jamaluddin, H., Rahman, R. A., Samin, P. M. Hudha, K. (2008). Vehicle Ride Performance With Semi Active Suspension System Using Modified Skyhook Algorithm and Current Generator Model. *International Journal of Vehicle Autonomous Systems, 2008.*

Liu, J., Li, X., Wang, Z., & Zhang, Y. (2016). Modelling and experimental study on active energy-regenerative suspension structure with variable universe fuzzy PD control. *Shock and Vibration*, *2016*.

Warake, K., Bhahulikar, S. R., & Satpute, N. V. (2018). Design & Development of Regenerative Braking System at Rear Axle. *International Journal of Advanced Mechanical Engineering*, *8*(2), 165-172.

Weforma Dämpfungstechnik GmbH. Weforma Triple Convolution Air Springs Data Sheet, 2014. Stolberg:Weforma, 2023. 3 p.

Zou, J., Guo, X., Xu, L., Tan, G., Zhang, C., & Zhang, J. (2017). Design, modeling, and analysis of a novel hydraulic energy-regenerative shock absorber for vehicle suspension. *Shock and vibration*, *2017*.

Zuo, L., & Zhang, P. S. (2013). Energy harvesting, ride comfort, and road handling of regenerative vehicle suspensions. *Journal of Vibration and Acoustics*, *135*(1), 011002.

## 6. RESPONSIBILITY NOTICE

The authors are the only ones responsible for the printed material included in this paper.